C. R. Mecanique 344 (2016) 715–724

Contents lists available at ScienceDirect

Comptes Rendus Mecanique

www.sciencedirect.com

Benchmark of different CFL conditions for IMPES

Comparaison de différentes conditions CFL pour l' IMPES

Jacques Franc [a,b,*], Pierre Horgue [a,b], Romain Guibert [a,b], Gerald Debenest [a,b]

[a] *Université de Toulouse, INPT, UPS, IMFT (Institut de mécanique des fluides de Toulouse), 2, allée du Professeur-Camille-Soula, 31400 Toulouse, France*
[b] *CNRS, IMFT, 31400 Toulouse, France*

ARTICLE INFO

Article history:
Received 21 March 2016
Accepted 16 August 2016
Available online 5 September 2016

Keywords:
IMPES
Stability criteria
CFL
Multiphase flow
Porous Media
Numerical Efficiency

Mots-clés :
IMPES
Critère de stabilité
CFL
Écoulements multiphasiques
Milieux Poreux
Efficacité numérique

ABSTRACT

The IMplicit Pressure Explicit Saturation (IMPES) method is a prevalent way to simulate multiphase flows in porous media. The numerical stability of this sequential method implies limitations on the time step, which may depend on the flow regime studied. In this note, three stability criteria related to the IMPES method, that differ in their construction on the observed variables, are compared on homogeneous and heterogeneous configurations for different two-phase flow regimes (viscous/capillary/gravitational). This highlights that there is no single optimal criterion always ensuring stability and efficiency. For capillary dominated flows, the Todd's condition is the most efficient one, while the standard Coat condition should be preferred for viscous flows. When gravity effects are present, Coat's condition must be restricted, but remains more efficient than the Todd's condition.

© 2016 Académie des sciences. Published by Elsevier Masson SAS. This is an open access article under the CC BY-NC-ND license (http://creativecommons.org/licenses/by-nc-nd/4.0/).

RÉSUMÉ

L'*IMplicit Pressure Explicit Saturation method* (IMPES) est l'une des principales méthodes pour traiter les cas d'écoulements multiphasiques en milieu poreux. La stabilité numérique de cette méthode séquentielle implique des contraintes différentes sur le pas de temps selon le régime d'écoulement étudié. Dans cette note, les trois principaux critères de stabilité liés à l'IMPES sont testés sur des milieux homogènes et hétérogènes pour différents régimes (visqueux/capillaire/gravitaire). Cette étude montre qu'aucun critère optimal, réunissant stabilité et efficacité, ne se dégage. Pour les écoulements capillaires, la condition de Todd est la plus efficace, tandis que la condition standard de Coats est préférable pour les écoulements visqueux. Quand les effets gravitaires sont pris en compte, la condition de Coats doit être restreinte, mais demeure plus efficace que celle de Todd.

© 2016 Académie des sciences. Published by Elsevier Masson SAS. This is an open access article under the CC BY-NC-ND license (http://creativecommons.org/licenses/by-nc-nd/4.0/).

* Corresponding author at: IMFT; 2 Allée Camille Soula, 31400 Toulouse, France.
E-mail addresses: jacques.franc@imft.fr (J. Franc), pierre.horgue@imft.fr (P. Horgue), romain.guibert@imft.fr (R. Guibert), gerald.debenest@imft.fr (G. Debenest).

http://dx.doi.org/10.1016/j.crme.2016.08.003
1631-0721/© 2016 Académie des sciences. Published by Elsevier Masson SAS. This is an open access article under the CC BY-NC-ND license (http://creativecommons.org/licenses/by-nc-nd/4.0/).

1. Introduction

Among the possible numerical methods used to simulate two-phase flow in porous media [1–3], the IMplicit Pressure Explicit Saturation (IMPES) method remains in use today [4,5]. This sequential algorithm, originally proposed by Sheldon [6], has the advantage to substantially reduce the size of the linear systems to solve, compared to a fully implicit method. In return, the method is limited by important numerical stability restrictions on the size of the time step. Hybrid methods, Adaptive Implicit Methods (AIM), have also been proposed and treat implicitly unknowns in regions with high throughput ratio [7].

The numerical instabilities are due to the non-linear effects involved in two-phase flow in porous media and mainly related to capillary pressure and relative permeability laws. The explicit resolution of saturation requires the linearization of capillary and permeability laws, which could lead to numerical instability. This can lead to erroneous calculations of the saturation field and, in the worst cases, to the end of the simulation (the computed saturation is out of the limits). The various laws and their complexity make stability even harder to predict, and therefore different stability criteria have been proposed and studied. Todd [8] has first derived a condition based on averaged spatial and temporal saturation variations, which provides an increasing/decreasing factor for the time step. Coats [9], through a proper Von Neumann analysis, has derived a CFL criteria based on mobility related terms, fluxes, and capillary pressure. One can also use the classical CFL [10] condition to ensure stability. Other stability studies have been conducted focusing on upstream scheme [11], on switching criteria for AIM [7,12], or on extension to compositional and black-oil models [13]. Even if Coats' stability criterion is commonly used, it may be very restrictive in certain circumstances and is therefore not necessarily the optimum choice. To our knowledge, there is no study in the literature comparing these different stability criteria to highlight their effectiveness for different porous media viscous flow regimes involving, or not, capillary and gravitational effects.

This need for numerical stability is all the more important as two-phase flows in porous media are often subject to physical instabilities. This class of instabilities can be caused by various configurations such as counter current flows and layered flows or by properties of the studied system (mobility ratio, viscosity ratio, permeability distribution). The most commonly known and studied instability is the viscous fingering phenomenon [14]. When one is interested in simulating this kind of physical instability, the numerical stability should be ensured to avoid the perturbation of the system by a numerical artifact.

In a recent work [15], the IMPES method has been implemented and developed in the open-source framework OpenFOAM [16,17]. This open-source implementation has been successfully employed in various fields, such as two-phase flow in structured bed packing [18] and waste management [19].

The scope of the paper is the performance benchmark of existing criteria taken from the literature. A methodology is set up to compare their efficiency in terms of computational cost (number of linear solver iterations) for various cases. This study has been designed for helping IMPES users that struggle with stability issues in choosing the most suited criteria for their simulation. Its ambition is not to develop a new criterion, but to gather user experiences on different configuration with different criteria. We proposed to cross-compare Todd's, Coats' and classical Courant–Friedrichs–Lewy's criteria listed above, for different flow regimes (viscous/capillary/gravitational) and for homogeneous and heterogeneous permeability fields without singularities (e.g., no wellbore model).

This note is organized in two parts. In the first one, two-phase flow equations for porous media are described, detailing the IMPES algorithm and presenting the three stability numbers investigated. We introduce the mathematical formulation of the different criteria, stating which phenomena are included in the theoretical form. In the second part, numerical experiments are performed to explore the different stability conditions on three classical configurations, and define their efficiency.

2. Two-phase flow and stability numbers

2.1. Mathematical model

Two-phase flows under investigation are assumed incompressible, viscous and isothermal. The wetting and non-wetting phases are respectively denoted "w" and "n". The mass conservation equation for each phase reads

$$\begin{aligned} \phi \frac{\partial S_{\mathrm{w}}}{\partial t} + \nabla \cdot \mathbf{u}_{\mathrm{w}} &= q_{\mathrm{w}} \\ -\phi \frac{\partial S_{\mathrm{w}}}{\partial t} + \nabla \cdot \mathbf{u}_{\mathrm{n}} &= q_{\mathrm{n}} \end{aligned} \tag{1}$$

with the obvious relationship

$$S_{\mathrm{w}} + S_{\mathrm{n}} = 1 \tag{2}$$

In these equations, S_α refers to saturation, ϕ is porosity, q_α is the mass source/sink term, and $\mathbf{u}_\alpha$ denotes the superficial velocity for each phase α. The latter are slow enough to be modeled by generalized Darcy's laws [20],

$$\mathbf{u}_\mathrm{w} = -\boldsymbol{K}\cdot\lambda_\mathrm{w}\left(\nabla p_\mathrm{n} - \rho_\mathrm{w}\mathbf{g} - \nabla p_\mathrm{c}\right)$$
$$\mathbf{u}_\mathrm{n} = -\boldsymbol{K}\cdot\lambda_\mathrm{n}\left(\nabla p_\mathrm{n} - \rho_\mathrm{n}\mathbf{g}\right) \tag{3}$$

where $\boldsymbol{K}$ is the permeability tensor intrinsic to the porous material, ρ_α is the fluid density and $\mathbf{g}$ the gravitational acceleration. The capillary pressure, p_c, i.e. the pressure difference between both phases, depends on saturation [21], and reads:

$$p_\mathrm{c}\left(S_\mathrm{w}\right) = p_\mathrm{n} - p_\mathrm{w} \tag{4}$$

The mobility λ_α is defined as

$$\lambda_\alpha = \left(\frac{k_{r,\alpha}(S_\mathrm{w})}{\mu_\alpha}\right)_{\alpha=w,n} \tag{5}$$

where μ_α is the fluid viscosity and $k_{r,\alpha}$ is the relative permeability function.

Many models exist in the literature to represent capillary pressure and relative permeabilities according to the saturation value [21–25]. In the present study, the well-established Brooks and Corey model [23] is used. With such a model, capillary pressure, p_c, and relative permeabilities, $k_{r,\alpha}$, read

$$\begin{aligned} p_\mathrm{c}\left(S_\mathrm{w}\right) &= p_{\mathrm{c},0}\, S_\mathrm{e}^{-\frac{1}{m}} \\ k_{r,n}\left(S_\mathrm{w}\right) &= k_{r,n_\mathrm{max}}\left(1 - S_\mathrm{e}\right)^{\frac{3m+2}{m}} \\ k_{r,w}\left(S_\mathrm{w}\right) &= k_{r,w_\mathrm{max}} S_\mathrm{e}^{\frac{3m+2}{m}} \end{aligned} \tag{6}$$

where $p_{\mathrm{c},0}$, k_{r,n_max} and k_{r,w_max} are model parameters and the pore-size index, m, is a characteristic number of the porous medium considered: small for large range pore-size distribution, large for relatively uniform pore-size distribution. The reduced saturation,

$$S_\mathrm{e} = \left(\frac{S_\mathrm{w} - S_{\mathrm{w,irr}}}{1 - S_{\mathrm{w,irr}} - S_{\mathrm{n,res}}}\right) \tag{7}$$

represents that amount of wetting phase that can flow. It depends on the irreducible wetting saturation, $S_{\mathrm{w,irr}}$ and the residual non-wetting saturation, $S_{\mathrm{n,res}}$.

2.2. IMPES algorithm

The chosen unknowns for the numerical implementation are the pressure of the non-wetting phase and the saturation of the wetting phase $(p_\mathrm{n}, S_\mathrm{w})$. The saturation S_w is governed by the wetting phase mass conservation Eq. (1) and the pressure p_n satisfies the global mass conservation,

$$\nabla\cdot\left(-\boldsymbol{K}\cdot\lambda_t\nabla p_\mathrm{n}\right) - \nabla\cdot\left(\boldsymbol{K}\cdot\Psi\left(\rho_\mathrm{w} - \rho_\mathrm{n}\right)\cdot\mathbf{g} - \boldsymbol{K}\cdot\Psi\, p_\mathrm{c}'\nabla S_\mathrm{w}\right) = q_\mathrm{t} \tag{8}$$

where $\lambda_\mathrm{t} = \lambda_\mathrm{w} + \lambda_\mathrm{n}$ is the total mobility, $q_\mathrm{t} = q_\mathrm{w} + q_\mathrm{n}$ is the total sink/source term and $\Psi = \frac{2\lambda_\mathrm{w}\lambda_\mathrm{n}}{\lambda_\mathrm{w}+\lambda_\mathrm{n}}$ is the harmonic average of mobilities. The first derivative of capillary pressure with respect to the wetting phase saturation S_w is introduced as $|p_\mathrm{c}'|$.

The IMPES solution algorithm consists in solving implicitly the pressure equation (8) and explicitly the saturation equation (1). The details of the implemented algorithm can be found in a previous work [15]. In the following simulations, a first-order upwind interpolation is used for mobility-related terms and a backward Euler scheme is adopted for time discretization.

The linear solver used in the experiment is a conjugate gradient solver with a diagonal incomplete Cholesky preconditioner. It is a commonly used pair when dealing with symmetric matrices. A generalized geometric–algebraic multi-grid solver might be an appropriate alternative for solving this equation over large domains. As the cases treated in the next section remain simple in terms of number of cells and considering that the solver's efficiency is not in the scope of this work, the choice of such a preconditioner–solver pair is not disadvantageous.

2.3. Stability criteria

In this section, the three tested CFL conditions ensuring the stability of IMPES simulations are described: namely the classic Courant number condition (Co), the Todd's derived number condition (T) and the Coats' derived number condition (C). For each criterion, a time-step factor F, which gives the increase or decrease in the time-step size during the simulation, is defined.

2.3.1. Classic Courant number condition (Co)

This condition limits the Courant number of each phase α by a user-defined value, $Co_{\max}$:

$$Co = \frac{1}{2}\max_{i,\alpha}\left(\frac{\sum_{\text{faces}\subset i}|q_{\alpha,f}|}{V_i}\Delta t\right) < Co_{\max} \qquad i = 1, N_{\text{cells}} \tag{9}$$

This Courant number is a direct adaptation of the classical one extended to two-phase flows [10]. It involves the sum of absolute values of fluxes in phase α through every face of cell i (term $\sum_{\text{faces}\subset i}|q_{\alpha,f}|$) and the volume V_i of the cell i. It is designed to ensure the stability of the hyperbolic saturation equation. The time-step factor F is defined as:

$$F = \frac{Co_{\max}}{Co} \tag{10}$$

2.3.2. Todd's number condition (T)

The first stability criterion dedicated to the IMPES algorithm [8] has been derived taking into account the discretized form of the pressure and saturation equations. It leads to a constraint on the time step, split into two time-step restrictions, according to whether capillary pressure p_c or relative permeabilities k_r is (are) considered:

$$\Delta t \le \min_i\left[\Delta t_{p_c,i}, \Delta t_{k_r,i}\right] \qquad i = 1, N_{\text{cells}} \tag{11}$$

The capillary restriction on the time step can be expressed as

$$\Delta t_{p_c,i} \le \frac{\phi V_i}{\left|p_c'\right|\sum_{\text{faces}\subset i}\left(T_f\Psi\right)} \qquad i = 1, N_{\text{cells}} \tag{12}$$

where $T_f = (KA/\Delta x)$ is the transmissivity of face f, whose area is noted A and whose distance to the cell center is noted Δx. Harmonic interpolation of K is chosen for computing transmissivity T_f. Equation (12), reformulated as a CFL condition, reads:

$$CFL_{\text{Todd,pc}} = \Delta t_{p_c,i}\frac{\left|p_c'\right|\sum_{\text{faces}\subset i}\left(T_f\Psi\right)}{\phi V_i} < CFL_{\text{Todd,max}}, \quad i = 1, N_{\text{cells}} \tag{13}$$

which introduces a user-defined upper limit $CFL_{\text{Todd,max}}$.

The relative permeability restriction, formulated in terms of inter-cell fluxes, reads

$$\Delta t_{k_r,i} \le \frac{\phi V_i}{f'_{\text{w,i}}\left(\sum_{\text{faces}\subset i}|q_f|\right)} \qquad i = 1, N_{\text{cells}} \tag{14}$$

with f'_{w} the derivative of the fractional flow $f_{\text{w}} = \frac{\lambda_{\text{w}}}{\lambda_{\text{t}}}$ with respect to the saturation of the wetting phase S_{w} and q_f the total flux through face f. In terms of spatial and temporal saturation variation, a time step ratio can be used, with the 1/2 factor depending on the chosen spatial discretization scheme (e.g., here 1-pt upwind in 1D):

$$T = \frac{\Delta t_{k_r}^{n+1}}{\Delta t_{k_r}^{\text{n}}} = \frac{1}{2}\frac{\frac{1}{N_{\text{cells}}}\sum_i|\Delta_{i,i+1}S_{\text{w}}|}{\max_i(|\Delta_{\text{t}}S_{\text{w}}|)} \qquad i = 1, N_{\text{cells}} \tag{15}$$

Here, equation (15) defines directly a time step factor referred to in the following as T number. The symbol $\Delta_{i,i+1}S_{\text{w}}$ stands for the difference between two neighboring cells and $\Delta_{\text{t}}S_{\text{w}}$ is the saturation difference between n and $n-1$ time states. The time-step factor F includes both parts, capillary pressure and relative permeability, and is defined as:

$$F = \min(T, \frac{CFL_{\text{Todd,max}}}{CFL_{\text{Todd,pc}}}) \tag{16}$$

2.3.3. Coats' number condition (C)

More recently, starting from inequality (12) and (14) using Neumann's stability analysis, a new stability number C has been developed [9]:

$$C = \max_f\left[\frac{\Delta t}{\phi V_{i|f}}\left(\frac{\lambda_{\text{n}}}{\lambda_{\text{t}}\lambda_{\text{w}}}\left|q_{\text{w},f}\right|\lambda'_{\text{w}} - \frac{\lambda_{\text{w}}}{\lambda_{\text{t}}\lambda_{\text{n}}}\left|q_{\text{n},f}\right|\lambda'_{\text{n}} + \left(T_f\Psi\right)\left(\left|p'_{\text{c},f}\right|\right)\right)\right] \le C_{\max} \qquad f = 1, N_{\text{faces}} \tag{17}$$

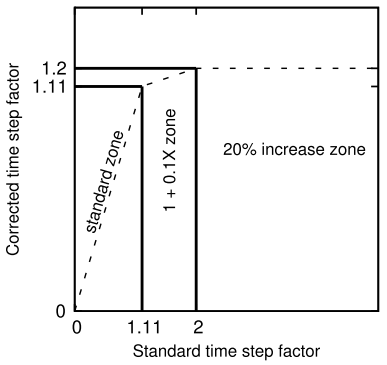

Fig. 1. Time-step evolution law.

where $C_{\max}$ is a user-defined limit. $V_{i|f}$ and $p'_{c,f}$ are respectively the linear interpolated values of the neighbor cell's volume and derivative of capillary pressure with respect to wetting phase saturation S_w. The C number includes all considered phenomena (gravity and capillarity) and their spatial variations to better spot local effects that could result in instability. The time-step factor F is defined as:

$$F = \frac{C_{\max}}{C} \tag{18}$$

It can be noted that if capillary and gravity effects are neglected, Coats' (C) and Todd's (T) conditions reduce to the same theoretical stability restriction. This is in agreement with other analyses [7,13]. However, in practice, Todd's number is computed from saturation variations, while Coat's one is computed from fluxes. This may result in large differences in terms of time-step computations, as observed in the Buckley–Leverett experiments.

2.4. Time-step increasing factor management

In order to improve stability and avoid large changes, the time step is computed as

$$\Delta t_{n+1} = \min\left(\min\left(F, 1 + 0.1F\right), 1.2\right) \Delta t_n \tag{19}$$

where F is the timestep factor defined for each stability number (Courant's, Coats' or Todd's). This approach is inherited from classical OpenFOAM solvers [16]. It limits the maximal increase to 20%, and reduces the increase between ~ 11 and 20%, as shown in Fig. 1. Note that this heuristic management mainly occurs at the beginning of the simulations, when saturation and pressure gradients are important. During the simulations, the variation of stability numbers is small between time iterations, and the upper bound of 1.10% is rarely reached.

3. Numerical experiments

In order to highlight the differences between the above stability criteria, simulations on well-known test cases are performed. We first consider a classical Buckley–Leverett experiment (viscous and gravitational regimes), then a 1D capillary rise experiment (capillary regime), and finally the 2D heterogeneous case (considering the three flow regimes) from [26]. Without other mentions, simulations are run with $k_{r,w_{max}} = 1$ and $k_{r,n_{max}} = 1$. Saturation limits are set with $S_{w,irr} = S_{n,res} = 0.001$. Brooks and Corey's m parameter is equal to $m = 5$. To assess the efficiency of stability criteria, the accumulated linear solver iterations, the computational effort required, are plotted as a function of the physical time of the simulated phenomenon. Indeed, the sole time step size data cannot render if the resolution is more or less time consuming. Some criteria can return a bigger time step, which makes it harder to solve the system for the linear solver. That is why the accumulated sum of the linear solver iterations is chosen. It provides a better idea of whether the system is fast or long to solve whatever the size of the time step, because linear solver iterations are directly proportional to the CPU time needed to invert the matrices.

Throughout the cases, ratio between viscous flux Φ_μ, gravitational flux $\Phi_{\mathbf{g}}$ and capillary flux Φ_{p_c} is given if relevant. The total flux Φ_t resulting from the pressure equation (8) is considered to be decomposed as

$$\Phi_t = \Phi_\mu + \Phi_{\mathbf{g}} + \Phi_{p_c} \tag{20}$$

highlighting the competition of the different phenomena driving the flow.

3.1. Buckley–Leverett experiments

The wetting phase is injected at $|u_{inj}| = 10^{-5}$ m·s^{-1} in the same direction as gravity acceleration with an absolute scalar permeability $K = 10^{-11}$ m^2. The gradient of capillary pressure is assumed to be null. Depending on the regime,

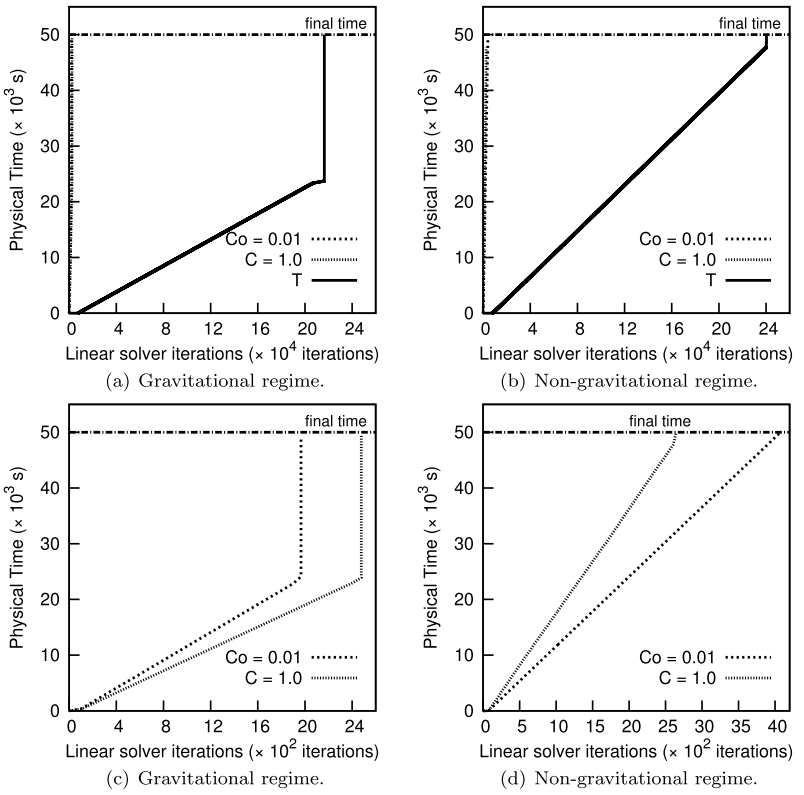

(a) Gravitational regime. (b) Non-gravitational regime.

(c) Gravitational regime. (d) Non-gravitational regime.

Fig. 2. Evolution of the accumulated linear solver iterations for the one-dimensional Buckley–Leverett experiment using the different stability criteria T, C and Co: (a,b) all stability criteria and (c,d) focusing C and Co criteria.

a semi-analytical solution can be calculated to predict the velocity and shape of the saturation front. This test highlights the relative permeability contribution to instability. In the gravitational case, the gravitational flux $\Phi_{\mathbf{g}}$ is 20 times greater than the viscous flux Φ_{μ}. The gravitational effects will set the front velocity.

Figs. 2(a)–2(b) show the accumulated linear solver iterations necessary to reach the final physical time and highlight that the T factor is clearly too restrictive for the Buckley–Leverett case and requires between 10 and 50 times more iterations. Equation (15) gives too restrictive time steps for 1D cases as mentioned in [8]. The criteria Co and C methods have similar time steps (Figs. 2(c)–2(d)) and involve almost the same computation time. However, we should note that contrary to the C factor, the Co method is case-dependent in the setting of its upper bound $Co_{\max}$ and, therefore, several tests were necessary to get the optimized value.

3.2. Capillary–gravity equilibrium experiment

In order to test the capillary pressure contribution for the different criteria, we perform simulations on a 1D vertical domain, whose lower half is filled with water (viscosity $\mu_{\mathrm{w}} = 10^{-3}$ Pa·s and density $\rho_{\mathrm{w}} = 1000$ kg·m^{-3}). The upper half is filled with air (viscosity $\mu_{\mathrm{w}} = 1.76\,10^{-5}$ Pa·s and density $\rho_{\mathrm{n}} = 1$ kg·m^{-3}). The capillary pressure parameter, $p_{\mathrm{c},0} = 1000$ Pa, has been tuned to balance gravity forces for this set of parameters. At the beginning of the simulation, the flow is mainly capillary-dominated, due to high saturation gradients until the equilibrium state between capillary and gravity forces is reached. In this configuration, the T-based method efficiency is close to that of the Co-based method (1.2 times faster), while the C method is 60 times slower, with an upper bound $C_{\max} = 1$ (see Fig. 3).

The maximum stable values of parameters $Co_{\max}$ and $C_{\max}$ for the tested cases and the related maximum time-step size reached during the simulations are reported in Table 1. It can be noticed that the Coats' criteria still ensure a stable simulation with values above the standard value ($C_{\max} = 1$) as observed in [9,27]. For the gravitational Buckley–Leverett experiment, the saturation front is very sharp and leads to a very restrictive maximum allowed time step of similar size with Co criteria. The same remark can be derived from the accumulated time steps in Fig. 2(c). For capillary–gravity equilibrium simulation, even though the maximal value of upper bound $C_{\max}$ is very high, the allowed time step is very restrictive. In such a configuration, Co and T criteria seem more appropriate.

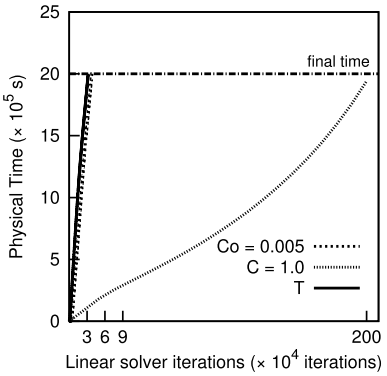

Fig. 3. Evolution of the accumulated linear solver iterations for the capillary rise configuration.

Table 1
Limits for $Co_{\max}$ and $C_{\max}$ parameters and maximum time step allowed on Buckley–Leverett and capillary rise cases.

	$Co_{\max}$	$C_{\max}$	$\Delta t_{Co,\max}(s)$	$\Delta t_{C,\max}(s)$	$\Delta t_{T,\max}(s)$
Non-gravitational Buckley–Leverett	0.15	1.19	37.49	65.25	0.18
Gravitational Buckley–Leverett	0.08	2.06	20	20.293	0.084
Capillary–gravity equilibrium	0.005	7.00	149.48	14.156	379.2

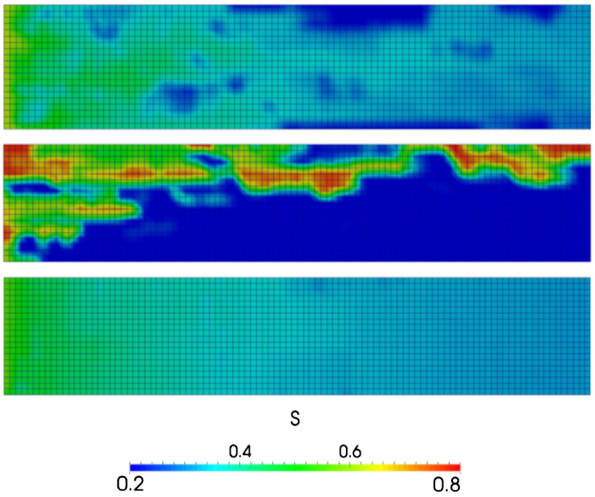

Fig. 4. Gas saturation field 2D SPE 10 case for the (top) non-gravitational, (middle) gravitational, and (bottom) capillary regimes.

3.3. SPE 10: 2D heterogeneous case

SPE 10th comparative solution project [26] proposed a two-dimensional heterogeneous permeability field more realistic than the academic cases previously used. The different stability numbers are tested out in non-gravitational, gravitational, and capillary regime. Phase densities and viscosities are given by the authors ($\rho_{\text{gas}} = 1$ and $\rho_{\text{oil}} = 700$ kg·m^{-3}, $\mu_{\text{gas}} = 10^{-5}$ and $\mu_{\text{oil}} = 10^{-3}$ Pa·s). Relative permeabilities and capillary pressure follow a Brooks and Corey law with coefficient $m = 5$. The case is an injection–production scenario: the gas is injected at the left side of the domain, oil and gas are produced at the right side. Without gravity (Fig. 4, top), the gas injected pushes the oil towards the production wellbore, while including gravity effects (Fig. 4, middle), oil and gas segregate because of the density difference, and gas overlays the oil present. Capillary effects, taken into account with $p_{c,0} = 0.1$ bar, tend to smooth saturation values. In order to have an easily readable representation of the prescribed domain, an aspect ratio of 0.2:2 is adopted. The accuracy of the numerical results are ensured by considering a L_2-norm error with $Co_{\max} = 5 \cdot 10^{-4}$ case as a reference. The configurations tested present a maximal relative error below 0.5%. Knowing that the discretization scheme is used in 2D, the T prefactor should be set to 0.25. However, the gravitational case is more challenging regarding stability, and T prefactor should be reduced in order to ensure the stability of the simulation as mentioned in [8]. In the gravitational case, the gravitational flux $\Phi_{\mathbf{g}}$ is 100 times greater than the viscous flux Φ_{μ} and, in capillary-dominated case, Φ_{p_c} is 500 times greater than Φ_{μ}.

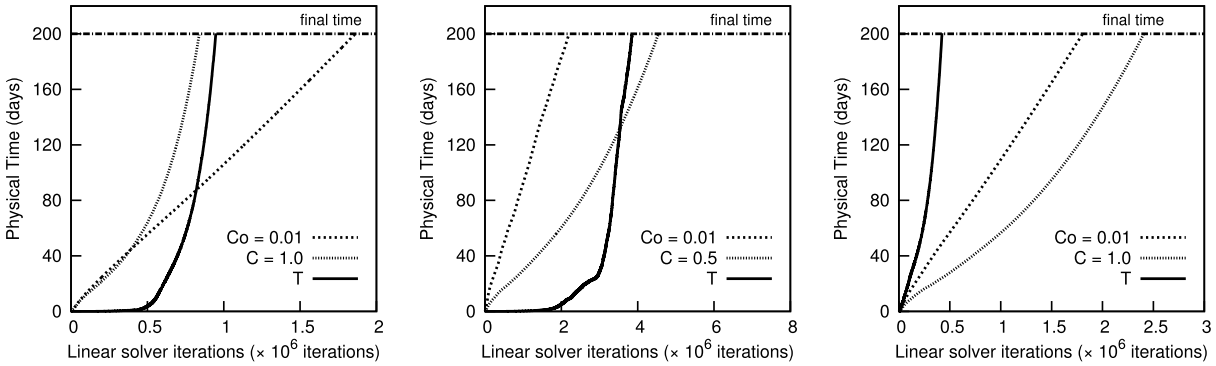

(a) Non-gravitational regime. (b) Gravitational regime. (c) Capillary regime.

Fig. 5. Evolution of the accumulated linear solver iterations for the SPE 10 2D.

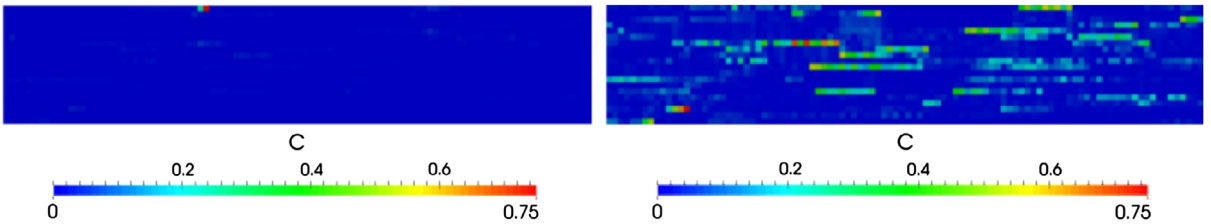

(a) Time 149 days. (b) Time 172 days.

Fig. 6. Uniform and non-uniform C number distribution in the gravitational regime.

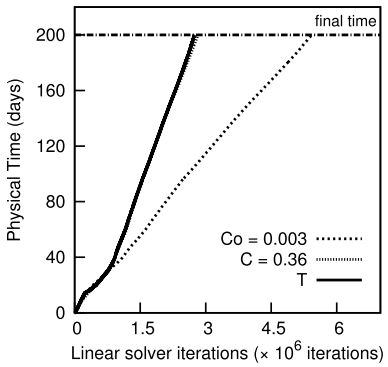

Fig. 7. Evolution of the accumulated linear solver iterations for the SPE 10 2D in the capillary–gravity regime.

The C and T methods lead to similar computation times in the non-gravitational case (cf. Fig. 5(a)), while Co leads to a simulation 2.2 times slower.

In the gravitational case, the criterion Co leads to the fastest resolution (reported in Fig. 5(b)), more than two times faster than the C criteria. This case illustrates what has been observed before in [9,27]. The C number could be either uniformly distributed throughout the domain and reaches its limit value only in one point (cf. Fig. 6(a)) or has a more non-uniform distribution with intermediate values and several points at the maximum value (cf. Fig. 6(b)). In the first case, the stability is critical and C provides a good approximation of a suitable time step to keep the simulation stable. In the second configuration, one can notice that C is too restrictive, and stability is still ensured for values beyond $C = 1$. Due to this change in repartition, C requires almost eight more linear solver iterations to solve the problem. The T method behaves slightly better with a 1.75 times faster simulation.

Similarly to the one-dimensional test cases, the capillary-driven case using the C number is the most complex in terms of stability and efficiency because it leads to unnecessary small time steps. This is also the case for Co-driven simulations because it requires to impose very a low maximum limit (here 10^{-2}). Regarding efficiency, T is the best criterion, as previously observed (Fig. 5(c)). Comparing the efficiency for this configuration, T is 4.25 times faster than Co and 6 times faster than C.

In the case where both capillary and gravitational effects are present, the T and C criteria lead to similar performances, while the Co produces a two-fold slower simulation (see Fig. 7).

Table 2
Limits for $Co_{\max}$ and $C_{\max}$ parameters and maximum time step allowed for the Buckley–Leverett and capillary rise cases.

	$Co_{\max}$	$C_{\max}$	$\Delta t_{Co,\max}(s)$	$\Delta t_{C,\max}(s)$	$\Delta t_{T,\max}(s)$
Non-gravitational	0.01	2.11	2445.3	27736	53290
Gravitational	0.01	0.56	2197	4925	7618
Capillary	0.01	3.63	2316	8583	49777
Capillary–gravity	0.003	0.36	667	1244	2512

As for the homogeneous porous medium, the maximum stable values of criteria C and Co are gathered in Table 2. These results highlight that Coats' number C allows the use of time steps from 2 to 10 times larger than those obtained with Co-driven simulations. The non-gravitational cross-flow exhibits $C_{\max}$ larger than the similar Buckley–Leverett experiment (2.11 instead of 1.19), which can be explained because of the non-uniform distribution of the maximum values of the criterion, as shown in Fig. 6. This configuration also occurs in capillary-dominated cases. When gravitational effects are included, with or without capillary effects, $C_{\max} = 1$ is no longer stable and should be reduced. Nevertheless, the latter criterion remains more efficient than the Co-driven simulation. The non-gravitational configuration is reported to be stable with a value of $C_{\max} = 2.0$ in [9].

For the challenging 2D cases that include gravity forces, Todd's criterion T has to be tuned to ensure stability. A prefactor δ is introduced as suggested in [8]. The values of this factor are respectively $\delta = 1/16$ for the gravity-driven case and $\delta = 1/32$ for the capillary–gravity case.

4. Conclusion

IMPES algorithm and its sequential structure still represent an interesting alternative to coupled approaches when treating problems with a challenging number of grid cells as required by highly detailed models. However, due to the specific form of conservative equations, the derivation of stability criterion more adapted than classic CFL condition is needed. Several contributions have tried to define more adapted saturation and pressure variation criteria [8], and on-going studies exist in the literature addressing this issue [9].

In this study, these various criteria have been compared with the classical Courant number in various conditions leading to the following observations. For homogeneous cases, the C method with limit set to $C_{\max} = 1$ will ensure stability in every configuration. For 2D heterogeneous cases, the C method faces two configurations:

- when the saturation front is diffuse, which is the case for capillary- or viscosity-dominated flows, it is safe to use a limit as $C_{\max} = 1$. However, it can be noted that the T method offers an interesting alternative, leading to a stable and fastest simulation. An alternative approach in the capillary-dominated cases is to switch to an implicit formulation, which suffers less from the loss of efficiency;
- when the saturation front is sharp, which is the case for gravity and capillary–gravity cases, phases are segregated and users have to limit the criterion to $C_{\max} = 0.25$, in order to keep the simulations stable. In the capillary–gravity configuration, the T method leads to similar performances as the C-method.

Even if Co-driven simulations can give better results in some cases, it remains a condition too dependent on the considered case. $Co_{\max}$ limit to be imposed for ensuring stability can differ by a factor of 1000 and makes this criterion unreliable. Following this work, it would be relevant to perform such a benchmark on the compressible formulation of IMPES or three-phase flows to confirm or invalidate the observations made in the frame of this study.

Acknowledgements

We thank ENGIE EP and STORENGY for their financial support to J. Franc.

References

[1] K. Aziz, A. Settari, Petroleum Reservoir Simulation, Applied Science Publishers Ltd., London, 1979.
[2] H. Cao, Development of Techniques for General Purpose Simulators, Stanford University Press, 2002.
[3] M.G. Gerritsen, L.J. Durlofsky, Modeling fluid flow in oil reservoirs, Annu. Rev. Fluid Mech. 37 (2005) 211–238.
[4] P. Mostaghimi, J.R. Percival, D. Pavlidis, R.J. Ferrier, J.L.M.A. Gomes, Anisotropic mesh adaptivity and control volume finite element methods for numerical simulation of multiphase flow in porous media, Math. Geosci. 47 (4) (2005) 417–440.
[5] A. Negara, A. Salama, S. Sun, Multiphase flow simulation with gravity effect in anisotropic porous media using multipoint flux approximation, Comput. Fluids 114 (2015) 66–74.
[6] J.W. Sheldon, W.T. Cardwell Jr, et al., One-Dimensional Incompressible Noncapillary Two-Phase Fluid Flow in a Porous Medium, Society of Petroleum Engineers, 1959.
[7] T.F. Russell, et al. Stability analysis and switching criteria for adaptive implicit methods based on the CFL condition, in: SPE Symposium on Reservoir Simulation, 6–8 February 1989, Houston, TX, USA.
[8] M.R. Todd, P.M. O'dell, G.J. Hirasaki, et al., Methods for Increased Ac curacy in Numerical Reservoir Simulators, Society of Petroleum Engineers, 1972.

[9] K.H. Coats, et al., IMPES stability: selection of stable timesteps, SPE J. 8 (02) (2003) 181–187, Society of Petroleum Engineers.
[10] R. Courant, K. Friedrichs, H. Lewy, Über die partiellen Differenzengleichungen der mathematischen Physik, Math. Ann. 100 (1928) 32–74.
[11] P.H. Sammon, et al., An analysis of upstream differencing, SPE Reserv. Eng. 3 (3) (1988) 1053–1056.
[12] P.A. Forsyth, Adaptive implicit criteria for two-phase flow with gravity and capillary pressure, SIAM J. Sci. Stat. Comput. 10 (2) (1989) 227–252.
[13] J. Wan, P. Sarma, A.K. Usadi, B.L. Beckner, et al., General stability criteria for compositional and black-oil models, in: SPE Reservoir Simulation Symposium, 31 January–2 Feburary 2005, The Woodlands, TX, USA.
[14] G.M. Homsy, Viscous fingering in porous media, Annu. Rev. Fluid Mech. 19 (1987) 271–311.
[15] P. Horgue, C. Soulaine, J. Franc, R. Guibert, G. Debenest, An open-source toolbox for multiphase flow in porous media, Comput. Phys. Commun. 187 (2014) 217–226.
[16] J. Hrvoje, Error analysis and estimation for the finite volume method with applications to fluid flows, PhD thesis, Department of Mechanical Engineering Imperial College of Science, Technology and Medicine, London, 1996.
[17] H.G. Weller, G. Tabor, H. Jasak, C. Fureby, A tensorial approach to computational continuum mechanics using object-oriented techniques, Comput. Phys. 12 (1998) 620–631.
[18] C. Soulaine, P. Horgue, J. Franc, M. Quintard, Gas–liquid flow modeling in columns equipped with structured packing, AIChE J. 60 (10) (2014) 3665–3674.
[19] A. Shewani, P. Horgue, S. Pommier, G. Debenest, X. Lefebvre, E. Gandon, E. Paul, Assessment of percolation through a solid leach bed in dry batch anaerobic digestion processes, Bioresour. Technol. 178 (2015) 209–216.
[20] M. Muskat, Physical Principles of Oil Production, McGraw Hill, New York, 1949.
[21] S.E. Buckley, M.C. Leverett, Mechanism of fluid displacement in sands, Trans. AIME 146 (1) (1941).
[22] J.H.M. Thomeer, et al., Introduction of a pore geometrical factor defined by the capillary pressure curve, J. Pet. Technol. 12 (3) (1960).
[23] A.T. Corey, R.H. Brooks, Drainage characteristics of soils, Soil Sci. Soc. Am. J. 39 (2) (1975) 251–255.
[24] M.T. Van Genuchten, A closed-form equation for predicting the hydraulic conductivity of unsaturated soils, Soil Sci. Soc. Am. J. 44 (5) (1980) 892–898.
[25] H.J. Morel-Seytoux, P.D. Meyer, M. Nachabe, J. Tourna, M.Th. Van Genuchten, R.J. Lenhard, Parameter equivalence for the Brooks–Corey and van Genuchten soil characteristics: preserving the effective capillary drive, Water Resour. Res. 32 (5) (1996) 1251–1258.
[26] M.A. Christie, M.J. Blunt, et al., Tenth SPE comparative solution project: a comparison of upscaling techniques, SPE Reserv. Eval. Eng. (2001) 308–317.
[27] K.H. Coats, et al., IMPES stability: the CFL limit, SPE J. 8 (3) (2003).